

IN-SILICO SCREENING OF PHYTOCHEMICAL COMPOUNDS IN *CAESALPINIA BONDUCELLA* L. SEEDS AGAINST THE GENE TARGETS OF OVARIAN STEROIDOGENESIS PATHWAY

Veerapandiyan Kandasamy¹, Sruthy Sathish², Thirumurthy Madhavan^{2*} and Usha Balasundaram^{1*}

Address(es):

¹ Department of Genetic Engineering, SRM Institute of Science and Technology, SRM Nagar, Kattankulathur -603 203, Kanchipuram, Chennai, Tamil Nadu, India.

² Computational Biology Laboratory, Department of Genetic Engineering, Faculty of Engineering and Technology, SRM Institute of Science and Technology, SRM Nagar, Kattankulathur-603203, Tamil Nadu, India.

*Corresponding author: sundaram.usha@gmail.com, thiru.murthyunom@gmail.com

<https://doi.org/10.55251/jmbfs.6124>

ARTICLE INFO

Received 2. 5. 2022
Revised 7. 6. 2023
Accepted 14. 6. 2023
Published 1. 10. 2023

Regular article



ABSTRACT

Polycystic ovary syndrome (PCOS) is the most common gynaecological disorder among reproductive-age women. Impaired metabolism of androgens and estrogens is one of the leading causes of PCOS. In India, medicinal herbs are being explored for their anti-androgenic and anti-estrogenic properties. In this study, we have screened the seed extracts of the herbal plant, *Caesalpinia bonducella* for potent inhibitors of estrogen and testosterone biosynthesis and assimilation. Methanol extract of *C. bonducella* seed kernels were subjected to gas chromatography - mass spectrometry (GC-MS) to identify the phytochemical constituents. Out of forty-three phytochemical compounds identified from the extract, eight compounds were selected based on Lipinski's rule of five for molecular docking. The selected phytochemical compounds were docked against specific targets of ovarian steroidogenesis pathway; human aromatase (*CYP19A1*), human 17 β -hydroxysteroid dehydrogenase type 1 (*HSD17B1*), human androgen receptor and estrogen receptor α . Further, the nature of these compounds was validated using density functional theory (DFT) calculations and ADME/T studies. As per the molecular docking output, compounds 33, 35, 38, 40, and 43 exhibited higher binding affinities against the four selected targets. Phytochemical compounds were optimized using Gaussian 16 with the B3LYP function and the 6-31G(d, p) basis set and were correlated with docking results. ADME/T helps in identifying the potential drug candidates from a pool of drugs. Five phytochemical compounds, 33, 35, 38, 40, and 43 were found to have the ability to bind and inhibit appropriate targets in the ovarian steroidogenesis pathway. Hence, these compounds can be further characterized *in vitro* and *in vivo* for alleviating PCOS.

Keywords: Polycystic ovary syndrome, *Caesalpinia bonducella*, Gas chromatography-mass spectrometry, Molecular docking and Density functional theory

INTRODUCTION

Polycystic ovary syndrome (PCOS) is one of the most common endocrine disorders among women of reproductive age, and about 1 in 10 women are affected by this disorder worldwide (Meier 2018). PCOS is diagnosed using Rotterdam criteria wherein, a woman may present any two of the following three clinical symptoms: hyperandrogenism, oligo/anovulation and an ultrasound imaging of polycystic ovaries. In the long run, PCOS patients gradually acquire other metabolic risks such as hypertension, cardiovascular disease, type 2 diabetes and obesity (Boyle and Teede, 2016; Dokras et al., 2017). Based on their biochemical presentations, women with PCOS are categorized into two groups: hormonal imbalance (HI) phenotype with dysregulated hormonal cycle and metabolic syndrome (MetS) phenotype with abnormal metabolic values (Janani and Usha 2020).

The MetS group, observed to be the significant phenotype among the Indian population, exhibits high levels of free testosterone indicating hyperandrogenism as the underlying pathology of PCOS. This group has high levels of blood glucose, insulin, cholesterol, HbA1C, and lower levels of High-density lipoprotein cholesterol (HDL-C). Hyper-insulinemic condition signals increased testosterone biosynthesis causing acne, obesity, Acanthosis nigricans and reduced follicle stimulating hormone (FSH) secretion and thus multiple premature follicles/cysts (Lerchbaum et al., 2014). In the hormonal imbalance phenotype, there is high estrogen (E2) level which raises luteinizing hormone (LH) secretion and decreases FSH secretion from the anterior pituitary. Low FSH level impedes the follicle stimulation, maturation and ovulation.

Secretion of FSH can be enhanced by reducing the E2 levels with inhibitors of aromatase enzyme (*CYP19A1* gene), that converts testosterone to estrogen (<https://www.ncbi.nlm.nih.gov/gene/1588>). Letrozole is the most widely used aromatase inhibitor with a 20-27% success in pregnancy (Holzer et al., 2006). FSH secretion from the pituitary can also be increased by blocking the estrogen receptors (ER α and ER β) with selective estrogen receptor modulators (SERM) like clomiphene citrate, raloxifene and tamoxifen (Xu et al., 2021; Homburg 2005). In case of hyperandrogenism, treatment to reduce hirsutism, acne and infertility is targeted at lowering the activity of the enzyme 17 beta-hydroxysteroid

dehydrogenases (encoded by *HSD17B1* gene) that catalyzes the conversion of androstenedione to testosterone and/or by inhibiting the androgen receptors (<https://www.ncbi.nlm.nih.gov/gene/3292>). Flutamide and spironolactone are well-known antagonists of androgen receptors, while decanoic acid inhibits the HSD enzyme (Paris and Bertoldo, 2019). Ovarian steroidogenesis pathway and the effective inhibitors of androgen and estrogen biosynthesis is illustrated in the figure 1. Although widely used, these antiestrogenic and anti-androgenic drugs stance some side effects such as hepatotoxicity (Conway et al., 2014), hot flushes, nausea, vomiting, impotence, vision problem and osteoporosis in PCOS patients (Sidra et al., 2019). Hence, phytomedicines from natural sources are continuously being investigated for PCOS.

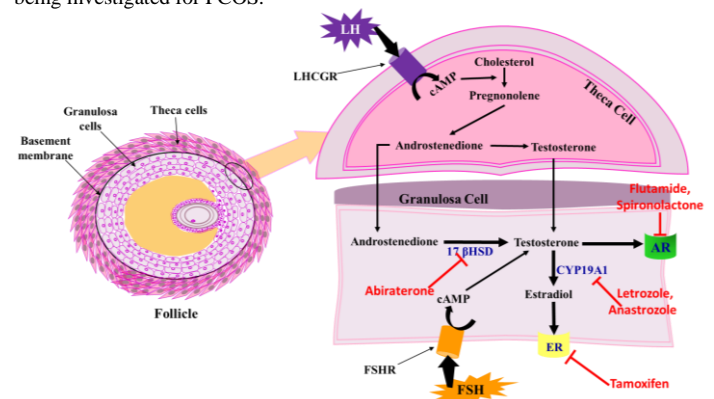


Figure 1 Representation of the inhibitory effect of commercially available drugs (red colour) on the genes and receptors of steroidogenesis pathway (blue colour).

Caesalpinia bonducella, a highly versatile medicinal shrub, is recently in the limelight to treat PCOS in India. *C. bonducella* L., also known as *C. bonducella* Flem. and *C. crista* Linn, belongs to the family of Caesalpinaceae. It

is commonly called bonduc nut, fever nut, and nicker nut (Khare 2007). The plant possesses anti-diabetic, hypolipidemic, antioxidant, anti-cancer, antipyretic and anti-inflammatory activities (Sachan et al., 2010; Sarma and Das, 2018, Shukla et al., 2009; Ihegwam et al., 2019; Shukla et al., 2010). More importantly, recent reports have demonstrated the antiestrogenic (Salunke et al., 2011) and anti-androgenic (Meerwal and Jain, 2016) potential of *C. bonducella* that has instigated us to identify the phytochemical compounds responsible for these activities.

Molecular docking and the conceptual density functional theory (DFT) approaches were used for validating the docking results of the compounds identified by GC-MS from *C. bonducella*. The phytochemical compounds derived from *C. bonducella* were docked against the targets, human aromatase (*CYP19A1*), human 17 β -hydroxysteroid dehydrogenase type 1 (*HSD17B1*), human androgen receptor and estrogen receptor alpha of ovarian steroidogenesis pathway. The interaction between target proteins and the phytochemical compounds were assessed based on their binding affinity. Further, the conceptual DFT and ADME/T studies were performed to render more knowledge on the chemical nature of these phytochemical compounds to facilitate further research on *in vivo* models.

MATERIALS AND METHODS

Plant sample collection

C. bonducella seeds were collected from Kolli hills (GPS code – 11°30'53.8"N 78°14'24.9"E), Namakkal District, Tamil Nadu, India. The seeds were brought to the laboratory and stored at room temperature for further use.

Sample preparation and solvent extraction

The seeds collected were cleaned and the outer seed coat was removed. The inner seed kernels that are widely used in the treatment of PCOS were shade dried for 10 - 15 days. Fifty grams of the ground seed kernels were added to 250 ml of methanol and was extracted using soxhlet apparatus for ten hours (5 cycles/hour) at 60 °C. The crude extracts obtained were filtered and the resulting solution was concentrated in a rotatory vacuum evaporator at 55 °C. The resultant crude sample was stored at 4 °C for GC-MS analysis and further experiments.

GC-MS analysis

Phytochemical investigation of seed kernel extracts of *C. bonducella* was performed in GC 7890B equipment connected to 5977A MS equipped with an autosampler (Agilent Technologies, USA). Concentrated and filtered extract of concentration 1 mg/ml, dissolved in methanol, was used for GC-MS analysis. The experimental conditions of GC-MS were as follows: HP-5MS 5% phenyl methyl siloxane capillary column with a dimension of 30 μm \times 250 μm \times 0.25 μm . The flow rate of the mobile phase with carrier gas helium was set at 1 ml/min with 70eV ionization energy in an electron impact mode. The sample injection volume was 1 μl , and the temperature programme (oven temperature) was 60 °C raised to 280 °C at the rate of 5 °C/min. The database namely the National Institute of Standards and Technology (NIST2011) was used to identify the unknown compounds by comparing them with the standard compounds reported earlier.

Preparation of protein

The 3D structures of the target proteins human aromatase (*CYP19A1*) (PDB ID: 3S79), human 17 β -hydroxysteroid dehydrogenase type 1 (*HSD17B1*) (PDB ID: 1FDS), human androgen receptor (PDB ID: 1E3G) and estrogen receptor α (PDB ID: 3ERT) were retrieved from the protein databank (PDB) (<https://www.rcsb.org/>). The 3D structure of the target proteins was visualized in PyMol software (<http://www.pymol.org>) and the H₂O molecules and associated ligands were removed initially. Furthermore, the target proteins' energy was minimized by adding charges to it using Autodock vina in PyRx software and the protein structure obtained was converted to pdbqt format for docking (Trott and Olson, 2009; Dallakyan and Olson 2015).

Ligands selection

The drug likeliness property of all the phytochemical compounds was investigated by the best-known physical property filters Lipinski's rule of five, using (<https://www.scfbio-iitd.res.in/utility/LipinskiFilters.jsp>) webserver. Lipinski's rule of five (molecular mass, number of hydrogen bond donors, and acceptors, log P and molar refractivity) was subjected to ligand preparation.

Preparation of ligands

The compounds selected based on Lipinski's rule of five were retrieved from the PubChem chemical database (<https://pubchem.ncbi.nlm.nih.gov/>). The ligand structures were uploaded to the PyRx open source software with OpenBabel plugin. The Spatial data file (SDF) of the ligands were converted to PDB format using the OpenBabel software (O'Boyle et al., 2011). Further, the structure of the

ligands was prepared by assigning charges, identifying the torsion root, correcting its angles and optimizing it using UFF (Universal force field). The generated ligand structures were converted to pdbqt format in order to generate 3D atomic coordinates of the molecules.

Active site prediction

The ligand can bind to many sites, but suitable ligand binding sites are defined from the ligands attached to the original target protein's active site. Active site residues were defined as atoms situated less than 25.0 °Å from any ligand atom (Ashraf et al., 2014). To identify the active sites, the structures of the target proteins were uploaded to the active site prediction server maintained by Supercomputing Facility for Bioinformatics and Computational Biology, Indian Institute of Technology, Delhi, to predict the probable ligand binding sites (<http://www.scfbio-iitd.res.in/dock/ActiveSite.jsp>).

Molecular docking

In this study, molecular docking was performed using Autodock vina in PyRx virtual screening open-source software maintained by the National Biomedical Computation Resources (Stouten and Kroemer; 2006; Kitchen et al., 2004; Vieira and Sousa, 2019). Four proteins and eight phytochemical compounds were selected under the vina wizard control for molecular docking. A grid appears over the target protein structure, and the grid size is adjusted based on the active site residues chosen. The docking was performed by Autodock vina and the strength of the interaction of the compounds and the target proteins was predicted based on the binding energy scores.

Conceptual DFT

Density functional theory (DFT) is a computational quantum mechanical modelling tool for examining the electronic structure of receptors and ligands, as well as the interactions between them. The electronic and structural parameters of the top ten hits were estimated using the B3LYP method and the 6-31G (d, p) basis set, with Gaussian 09 (Jordaan et al., 2020). Lowest unoccupied molecular orbital (LUMO), total energy, highest occupied molecular orbital (HOMO), global softness, energy gap, absolute hardness, molecular dipole moment, electrophilicity index, electronegativity and chemical potential were among the estimated parameters evaluated (Kulkarni et al., 2020).

ADME/T analysis

Poor ADME/T and pharmacokinetic properties can lead to the drug failure in experimental studies in the beginning or at lateral stage. So, early prediction of ADME/T properties can be useful in drug discovery (Panwar and Singh, 2021). The SDF (Structure Data Format) files and SMILES (Simplified Molecular-Input Line-Entry System) of the phytochemical compounds were retrieved from PubChem database for ADME/T analysis. The ADME/T (absorption, distribution, metabolism, excretion, and toxicity) properties of the chosen ligands were detected to understand their pharmacokinetic properties and their pharmacodynamic effects on the body. Analysis of ADME/T properties was done using the SwissADME (<http://www.swissadme.ch/>) and ADMET lab server (<http://admet.scbdd.com>).

RESULTS AND DISCUSSION

GC-MS analysis

After successful conventional soxhlet extraction, GC-MS analysis led to the identification of various compounds in the seed kernels of *C. bonducella*. The GC-MS chromatogram (Figure 2) recorded a total of 49 peaks which indicated the presence of 43 bioactive compounds with different retention times and percentage peak areas (Table 1).

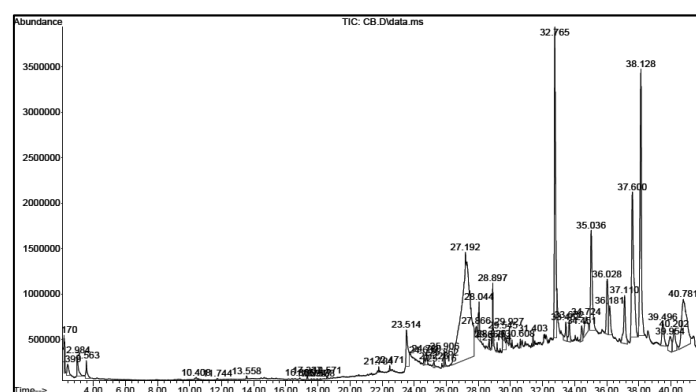


Figure 2 The GC-MS chromatogram of the methanol seed kernel extract of *C. bonducella*.

Table 1 GC-MS data of the phytochemicals present in *C. bonducella* methanol seed kernel extract

Peak	R.T. min	Molecular formula	Area %	Compounds	Compound number
1	2.17	C ₁₈ H ₃₅ BrO	1.05%	Octadecanal, 2-bromo-	1
2	2.399	C ₂ H ₄ OS	0.53%	Thioacetic acid	2
3	2.984	C ₃ H ₆ O ₂	0.88%	2-Propanone, 1-hydroxy-	3
4	3.563	C ₅ H ₁₀ O ₂	0.68%	Isopropyl acetate	4
5	10.408	C ₁₂ H ₂₆	0.14%	2,6-Dimethyldecane	5
6	11.744	C ₉ H ₂₀	0.04%	Hexane, 2,3,4-trimethyl-	6
7	13.558	C ₉ H ₂₀ O ₂ Si	0.07%	Silane, cyclohexyldimethoxymethyl-	7
8	16.866	C ₂₆ H ₅₄	0.03%	Octadecane, 3-ethyl-5-(2-ethylbutyl)-	8
9	17.337	C ₁₅ H ₃₂	0.11%	Dodecane, 2,6,11-trimethyl-	9
10, 11,	17.572,	C ₂₃ H ₄₈	0.03%,	Heptadecane, 9-hexyl-	10
12	17.757,		0.02%		
	17.947				
13	18.138	C ₁₇ H ₃₆	0.02%	Tetradecane, 2,6,10-trimethyl-	11
14	18.571	C ₂₁ H ₄₄	0.07%	Heptadecane, 2,6,10,14-tetramethyl-	12
15	21.784	C ₁₅ H ₃₂	0.07%	Dodecane, 2,6,11-trimethyl-	13
16	22.471	C ₁₄ H ₂₂ O	0.10%	Phenol, 2,4-bis(1,1-dimethylethyl)-	14
17	23.514	C ₁₂ H ₁₄ O ₄	2.16%	Diethyl Phthalate	15
18	24.602	C ₁₆ H ₃₀ O ₂	0.25%	2-Propenoic acid, tridecyl ester	16
19	24.78	C ₂₀ H ₃₄ O ₄	0.39%	5,9-Tetradecadienedioic acid, 5,6,9,10-tetramethyl-, dimethyl ester	17
20	25.226	C ₂₆ H ₅₄	0.19%	Octadecane, 3-ethyl-5-(2-ethylbutyl)-	18
21	25.716	C ₁₆ H ₃₂ O	0.05%	Hexadecen-1-ol, trans-9-	19
22, 23	25.862,	C ₁₄ H ₂₂ O ₄	0.13%,	2,8-Decadienedioic acid, diethyl ester	20
	25.906		0.31%		
24	27.192	C ₇ H ₁₄ O ₆	28.14%	3-O-Methyl-d-glucose	21
25	27.866	C ₁₈ H ₃₆ O ₂	0.43%	Hexadecanoic acid, ethyl ester	22
26	28.044	C ₁₈ H ₂₄ O ₂	1.16%	5,8,11-Heptadecatriynoic acid, methyl ester	23
27	28.668	C ₂₁ H ₃₀ O ₂	0.22%	5,8,11-Eicosatriynoic acid, methyl ester	24
28	28.82	C ₁₆ H ₃₂ O	0.20%	Hexadecen-1-ol, trans-9-	25
29	28.897	C ₁₉ H ₃₄ O ₂	0.89%	9,12-Octadecadienoic acid, methyl ester	26
30	29.164	C ₁₉ H ₃₈ O ₂	0.19%	Heptadecanoic acid, 16-methyl-, methyl ester	27
31	29.545	C ₁₈ H ₃₂ O ₂	1.15%	17-Octadecynoic acid	28
32	29.927	C ₁₆ H ₃₀ O	0.28%	Cyclopropane, 1-(1-hydroxy-1-heptyl)-2-methylene-3-pentyl-	29
33	30.608	C ₁₅ H ₂₉ BrO	0.13%	14-Bromo-2-methyltetradec-1-en-3-ol	30
34	31.403	C ₂₀ H ₄₀ O ₂	0.16%	Hexadecanoic acid, butyl ester	31
35	32.765	C ₁₉ H ₃₈ O ₄	11.13%	Hexadecanoic acid, 2-hydroxy-1-(hydroxymethyl) ethyl ester	32
36	33.452	C ₂₀ H ₂₅ NO ₃ S	0.80%	Androst-4-en-11-ol-3,17-dione, 9-thiocyanato-	33
37	33.662	C ₃₅ H ₆₈ O ₅	0.81%	Hexadecanoic acid, 1-(hydroxymethyl)-1,2-ethanediy ester	34
38	34.451	C ₂₁ H ₃₀ O ₅	0.62%	Pregn-5-ene-12,20-dione, 3,14,15-trihydroxy-, (3β,14β,15α)-	35
39	34.724	C ₂₁ H ₄₀ O ₄	1.48%	9-Octadecenoic acid (Z)-, 2-hydroxy-1-(hydroxymethyl) ethyl ester	36
40	35.036	C ₂₁ H ₄₂ O ₄	5.13%	Octadecanoic acid, 2-hydroxy-1-(hydroxymethyl) ethyl ester	37
41, 42	36.028,	C ₂₀ H ₂₈ O ₃	2.59%,	6β-Hydroxymethandienone	38
	36.181		1.39%		
43	37.11	C ₂₂ H ₃₂ O ₅	2.69%	1-Phenanthrenecarboxylic acid, tetradecahydro-7-(2-methoxy-2-oxoethylidene)-1,4a,8-trimethyl-9-oxo-, methyl ester	39
44	37.6	C ₂₂ H ₃₂ O ₃	9.65%	17Alpha-ethynyl-6beta-methoxy-3alpha,5-cyclo-5alpha-androstane-17beta,19-diol	40
45, 46,	38.128,	C ₂₆ H ₃₆ O ₈	11.56%,	1H-Cyclopropa [3,4] benz[1,2-e] azulene-5,7b,9,9a-tetrol,	41
48	39.496,		1.55%,	1a,1b,4,4a,5,7a,8,9-octahydro-3-(hydroxymethyl)-1,1,	
	40.202		1.56%	6,8-tetramethyl-, 5,9,9a-triacetate,	
47	39.954	C ₁₉ H ₂₂ N ₂	1.15%	Benzimidazole, 2-[1-(4-isopropylbenzyl) ethyl]-	42
49	40.781	C ₂₅ H ₃₄ O ₅	7.58%	Acetic acid, 17-(1-acetoxy-ethyl)-10,13-dimethyl-3-oxo-2,3,8,9,10,11,12,13,14,15,16,17-dodecahydro-1H -cyclopenta[a]phenanthren-11-yl (ester)	43

The peak area percentage that depicts the weight percentage ratio of the particular compound in the mixture was investigated, and eight phytochemical compounds were found to be abundant. Among the identified compounds, compound 21 had the maximum area percentage of 28.14%, followed by compound 41 (11.56%), compound 32 (11.13%), compound 40 (9.65%), compound 43(7.58%), compound 37(5.13%), compound 39 (2.69%) and compound 38 (2.59%). Other compounds present in the methanol extract were in minimal amounts, as shown in table 1.

Some steroid group compounds have been detected and reported as a result of this GC-MS analysis. A steroid compound 33 at RT (33.452) was detected in our GC-MS result, and this compound was previously reported in the n-hexane crude extract of *Boleophthalmus boddarti* by GC-MS analysis (Ridho et al., 2020). A steroid compound was identified in a study on *Digitalis purpurea* L. leaves that is similar to our compound 35 at RT (34.451), and the structure of the compound was also reported (Satoh and Morita, 1968).

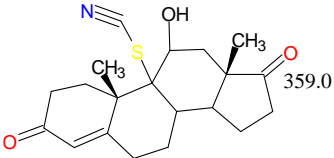
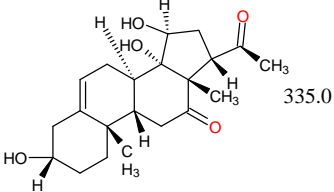
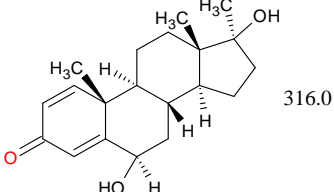
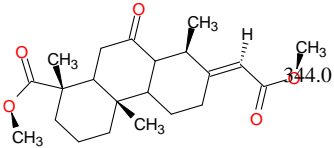
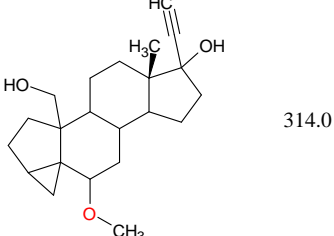
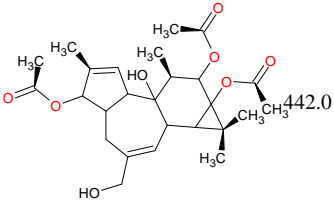
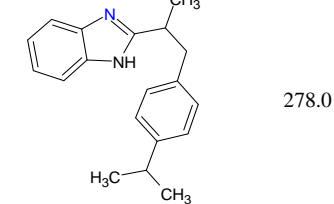
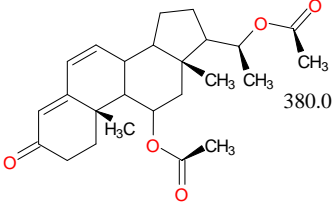
A study on bovine hepatocytes using GC-MS have identified the compound that is similar to the compound 38 in our GC-MS analysis. In that study, they used standard 6β-hydroxymethandienone for identification of our desired compound (compound 38) and other metabolites also identified from calves' urine samples (Hooijerink et al., 1998). Compound 39 showed in chloroform extract of *Melilotus indicus*, and it showed the alpha-amyrase and lipase inhibitory activities (Iftikhar et al., 2019). Compound 41 retention time 38.128, 39.496 and 40.202 then major peak area percentage of 11.56. 6β-Hydroxymethandienone compound has been already reported in the *Taxus chinensis* plant and confirmed its presence by GC-MS (Hu et al., 2020). PCOS can be treated by natural compounds that have high pharmacological activity that regulate androgen and estrogen levels.

Selection of the ligands

From the GC-MS analysis, only eight out of forty-three phytochemical compounds satisfied the Lipinski rule of five. The main goal to verify Lipinski rule is to obtain a preliminary prediction of the potential pharmacological capacities of a molecule

to become a drug (Bouzekri et al., 2022). Therefore, the compounds listed in Table 2 were used as ligands for molecular docking with target proteins. Investigation of drug-likeness properties accelerates the process of drug discovery and development.

Table 2 Compounds selected based on Lipinski's rule of five

Compound number	Compound structure	Mass (less than 500)	Hydrogen bond donor (less than 5)	Hydrogen bond acceptors (less than 10)	LOGP (less than 5)	Molar refractivity (should be between 40 and 130)
Compound 33		359.0	1	4	3.3	95.5
Compound 35		335.0	3	5	-0.1	83.8
Compound 38		316.0	2	3	3.0	88.6
Compound 39		344.0	0	5	0.7	83.0
Compound 40		314.0	2	3	0.1	79.6
Compound 41		442.0	2	8	-1.1	108.9
Compound 42		278.0	1	1	5.0	88.7
Compound 43		380.0	0	5	0	97.5

Active site characterization

Human aromatase (PDB: 3S79), human 17β-hydroxysteroid dehydrogenase type 1 (PDB: 1FDS), human androgen receptor (PDB ID: 1E3G) and estrogen receptor α (PDB: 3ERT) active sites as recommended by the literature matched with the SCFBio active site prediction server as well. Our results show that the binding active site residues of human aromatase (*CYP19A1*) were shown in figure 3. Human 17β-hydroxysteroid dehydrogenase type 1 (*HSD17b1*) active site residues are clearly shown in figure 4, 5 and 6 shows the binding active site residues of human androgen and estrogen receptor α respectively.

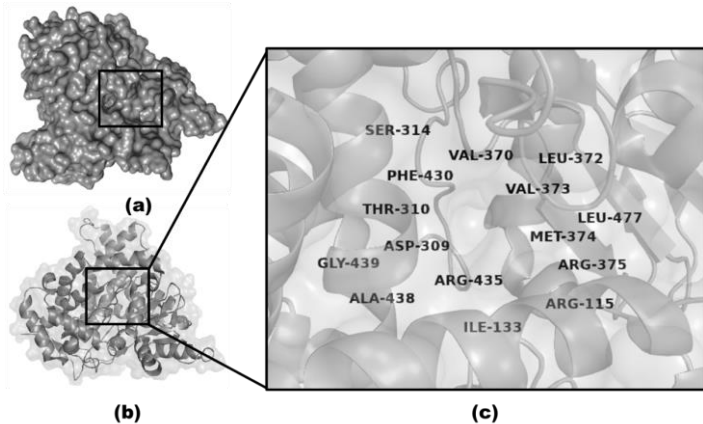


Figure 3 Active site for ligands in human aromatase (*CYP19A1*). The bind site representing the (a) surface, (b) chains and (c) cavity enlarged to unveil the amino acid residues interacting in <5.0 Å vicinity.

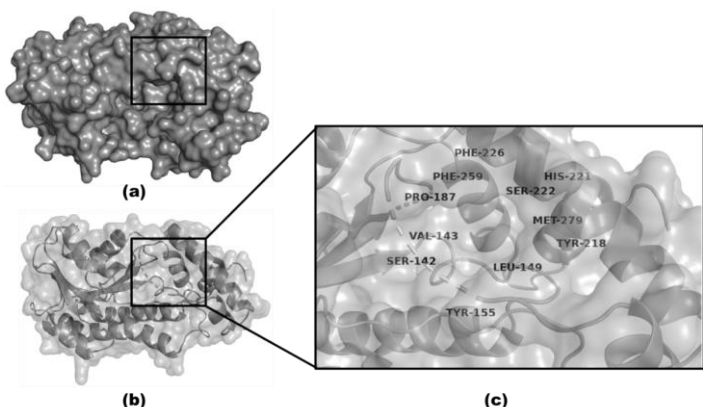


Figure 4 Active site for ligands in human 17β-hydroxysteroid dehydrogenase type 1 (*HSD17b1*). The bind site representing the (a) surface, (b) chains and (c) cavity enlarged to unveil the amino acid residues interacting in <5.0 Å vicinity.

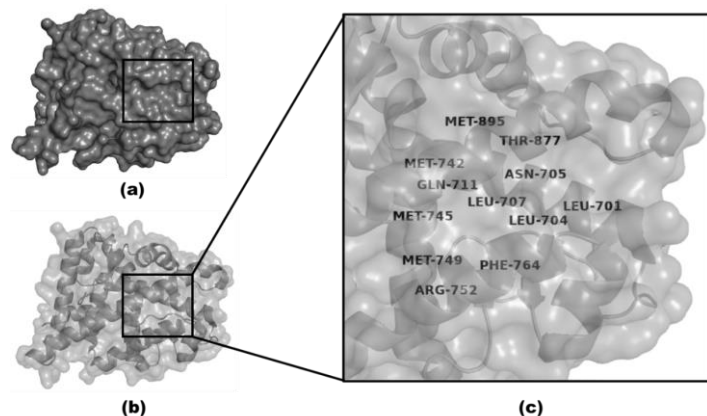


Figure 5 Active site for ligands in human androgen receptor. The bind site representing the (a) surface, (b) chains and (c) cavity enlarged to unveil the amino acid residues interacting in <5.0 Å vicinity.

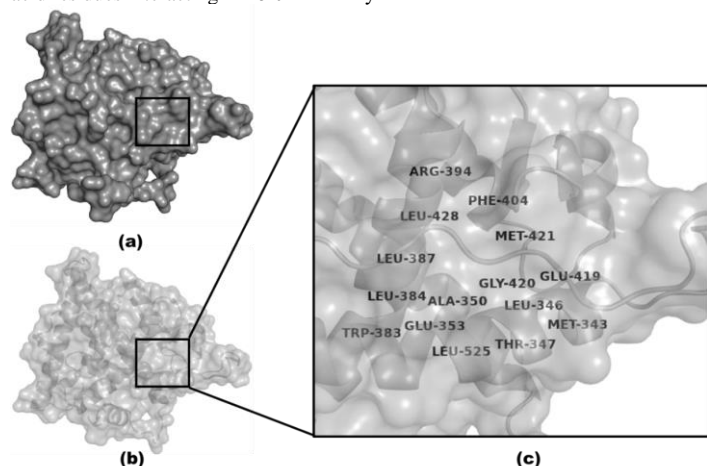


Figure 6 Active site for ligands in estrogen receptor α. The bind site representing the (a) surface, (b) chains and (c) cavity enlarged to unveil the amino acid residues interacting in <5.0 Å vicinity.

Molecular docking

The selected compounds were docked with the target proteins human aromatase (*CYP19A1*), human 17β-hydroxysteroid dehydrogenase type 1 (*HSD17b1*), human androgen and estrogen receptor α) to identify the binding affinities of the compounds. In docking, the RMSD value is used to compare the docked conformation to the reference or other docked conformations. During the docking analysis, the most least RMSD value was selected from all conformations generated. The ligand and protein complex with hydrogen and hydrophobic interactions and binding energies are shown in Table 3.

Table 3 Docking score of the selected eight phytochemicals

PDB CODE	Compound number	Binding energy (kcal/mol)	Hydrogen bond interactions	Hydrophobic interactions
3S79 Human aromatase	Compound 33	-8.5	Ala438, Gly439	Ile133, Phe134, Trp224, Ala306
	Compound 35	-8.7	Thr310, Ala438, Gly439	Ile133, Trp224, Val370
	Compound 38	-8.8	-	Ile132, Ile133, Phe134, Trp224, Ala306, Ala438
	Compound 39	-8.8	Thr310, Ser314, Val370	Thr310, Val370, Phe430
	Compound 40	-8.5	Arg115	Ile132, Trp224, Ala306, Thr310, Val370, Ala438, Leu477
	Compound 41	-8.6	Arg115, Thr310	Ile132, Ile133, Phe148, Phe221, Trp224, Glu302, Ala306, Thr310, Leu477
	Compound 42	-8.4	-	Ile132, Phe148, Leu152, Glu302, Ala306, Ala307, Val370, Phe430
	Compound 43	-9.0	Arg115	Ile133, Trp224, Thr310, Val370, Ala438

Continue Table 3

1FDS HSD17b1	Compound 33	-7.6	Ser142, Tyr155	Leu96, Phe226
	Compound 35	-8.5	Asn152, His221	Leu149, Tyr, Val225, Phe226
	Compound 38	-7.9	-	Tyr155
	Compound 39	-8.8	-	Leu149, Tyr155, Phe226
	Compound 40	-7.3	Tyr218	Tyr155, Pro187
	Compound 41	-7.2	Val196	Leu96, Tyr155, Phe226
	Compound 42	-8.1	-	Val143, Leu149, Pro187, Val225, Phe226
	Compound 43	-7.1	Ser222	Leu96, Val143, Leu149, Tyr155, Pro187, Phe226
1E3G Human androgen receptor	Compound 33	-8.3	Thr877	Leu704, Leu707, Met745, Leu873, Phe876
	Compound 35	-7.0	Asn705, Gln711, Arg752	Leu704, Leu707, Met745, Met749, Phe764, Phe876
	Compound 38	-5.6	Gln711, Arg752	Leu704, Leu707, Met745, Phe764, Phe876
	Compound 39	-2.0	Gln711, Arg752	Leu704, Met745, Phe764, Phe876
	Compound 40	-3.8	-	Leu701, Met745, Met749, Phe764, Leu873, Phe876, Leu880
	Compound 41	-0.7	Gln711	Leu701, Leu704, Leu707, Met745, Val746, Met749, Phe764, Leu873, Phe876, Thr877, Leu880, Ile899
	Compound 42	-7.0	-	Leu701, Leu704, Leu707, Met745, Met749, Phe764, Leu873, Phe876, Leu880, Phe891
	Compound 43	-1.0	-	Leu704, Trp741, Met745, Val746, Phe764, Leu873, Phe876, Leu880
3ERT Human estrogen receptor alpha	Compound 33	-8.6	Arg394, His524	Leu346, Leu349, Leu387, Leu391, Phe404, Leu525
	Compound 35	-8.0	Glu353, Arg394, His524	Leu349, Ala350, Leu384, Leu387, Leu391, Ile424, Leu525
	Compound 38	-8.8	Arg394, His524	Leu346, Leu349, Ala350, Leu384, Leu387, Leu391, Phe404, Ile424, Leu525
	Compound 39	-5.0	-	Leu346, Ala350, Trp383, Leu384, Leu387, Leu525
	Compound 40	-7.8	-	Leu346, Ala350, Leu384, Leu387, Leu391, Phe404, Ile424, Leu525
	Compound 41	-3.2	-	Leu346, Thr347, Leu349, Ala350, Trp383, Leu384, Leu387, Leu391, Phe404, Leu428, Leu525
	Compound 42	-8.7	-	Leu346, Leu349, Trp383, Leu384, Leu391, Phe404, Ile424, Leu525
	Compound 43	-5.0	His524	Leu346, Leu349, Trp383, Leu384, Leu391, Phe404, Leu525

The compounds selected for visualization based on docking results are mentioned in bold

Protein docking results of human aromatase (*CYP19A1*) revealed compound 35 (-8.7 kcal/mol), compound 39 (-8.8 kcal/mol) and compound 43 (-9.0 kcal/mol) to have a good binding affinity (with hydrogen bond and hydrophobic bond interaction) with a better docking score among the eight compounds. Compounds 35, 39, 43 showed hydrogen bonding interaction with the amino acid residues Arg115, Thr310, Thr310, Ser314, Val370, Ala438 and Gly439. The docked position of individual top three ligands in human aromatase (*CYP19A1*) is shown in figure 7. For better visualisation, they have been represented in different colours. Compounds 35, 39 and 43 showed potential binding affinities to the targets. Additionally, these compounds also had better binding scores and hydrogen bond

interactions. Another study also demonstrated that the native ligand of androstenedione (ASD) docked against the human aromatase (*CYP19A1*) protein in polar and non-polar interactions, matched our present findings (Kumavath et al., 2016).

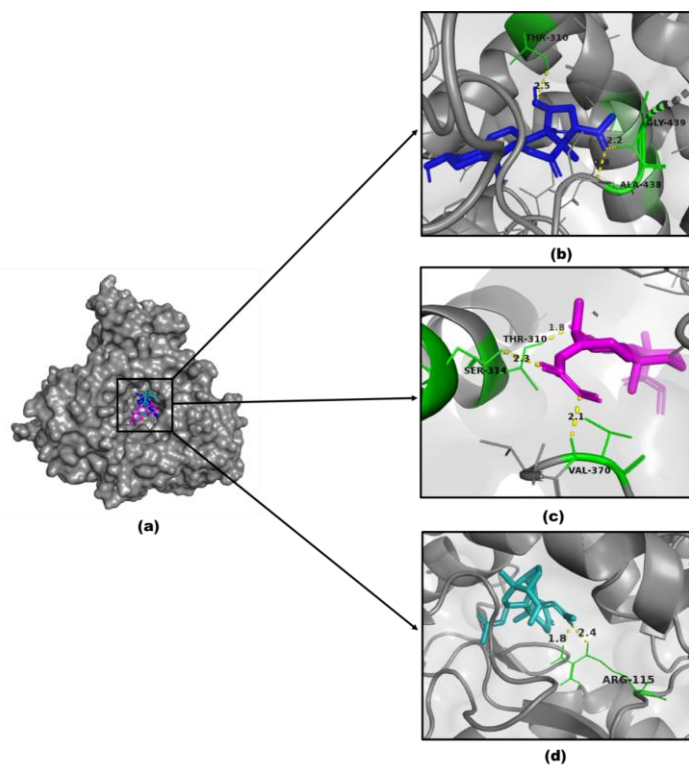


Figure 7 (a) The binding poses of compound 35 (blue), compound 39 (magenta) and compound43 (teal) to human aromatase (*CYP19A1*) (b) compound 35 interacting with the residues, Thr310, Ala438 and Gly439 (green) forming hydrogen bonds (yellow) of length 2.5 Å, 2.8 Å and 2.2 Å, respectively (c) compound 39 interacting with the residues, Thr310, Ser314 and Val370 (green) forming hydrogen bonds (yellow) of length 1.8 Å, 2.3 Å and 2.1 Å, respectively and (d) compound 43 interacting with the residues, Arg115 (green) forming hydrogen bonds (yellow) of length 1.8 Å, and 2.4 Å.

Similarly, when human 17 β -hydroxysteroid dehydrogenase type 1 (*HSD17B1*) protein was docked with the ligands, compound 33 (-7.6 kcal/mol), compound 35 (-8.5 kcal/mol) and compound 40 (-7.3 kcal/mol) displayed better docking score among all the compounds. The value showed hydrogen bonding with the amino acid residues Ser142, Asn152, Tyr155, Val196, Tyr218, His221 and Ser222 among all the conformations generated. The binding poses of the top ligands in the active site of *HSD17B1* are depicted in figure 8. The amino acid residues observed in the active site of this protein was in concordance with the 17 β hydroxysteroid dehydrogenase type 1 active site (Ser 142, Tyr 155, His 221) when a phytoestrogen compound (Estra1,3,5(10)-triene-16-acetamide, 3-hydroxy-17-oxoN-(3-pyridinylmethyl)-, (16 β)-methyl) was used as a ligand and this ligand interaction reduced the testosterone estradiol biosynthesis and decreased the endogenous bioavailability of testosterone and estradiol (Singla and Jaitak, 2015). Therefore, the compounds 33, 35, 40 reported in this study might effectively reduce the biosynthesis of testosterone and estradiol.

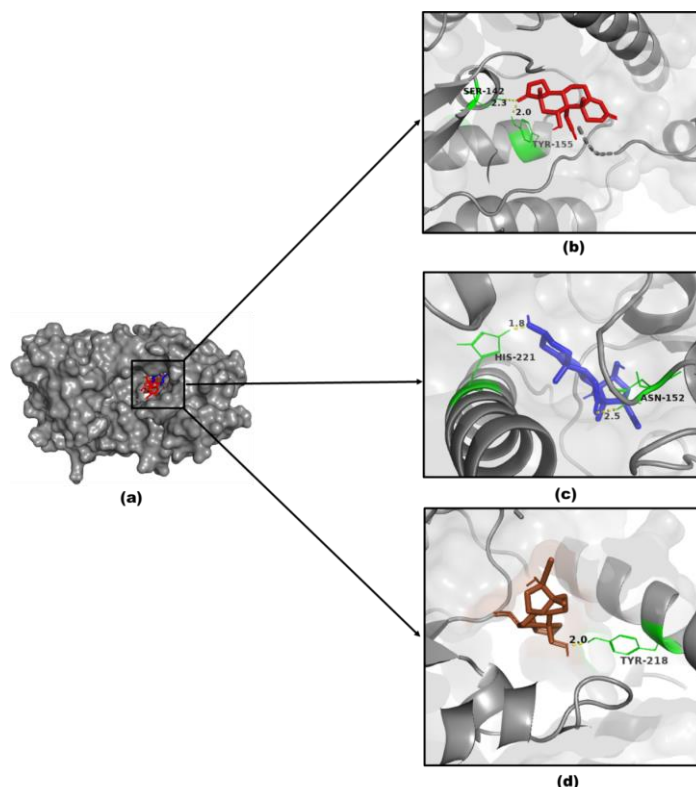


Figure 8 (a) The binding poses of compound 33 (red), compound 35 (blue) and compound40 (brown) to human 17-beta-hydroxysteroid-dehydrogenase type 1 (*HSD17b1*) (b) compound 33 interacting with the residues, Ser142 and Tyr155 (green) forming hydrogen bonds (yellow) of length 2.3 Å and 2.0 Å, respectively (c) compound 35 interacting with the residues, Asn152 and His221 (green) forming hydrogen bonds (yellow) of length 2.5 Å and 1.8 Å, respectively (d) compound 40 interacting with the residues, Tyr218 (green) forming hydrogen bonds (yellow) of length 2.0 Å.

Further, docking of human androgen receptor revealed that the compound 33 (-8.3 kcal/mol), compound 35 (-7.0 kcal/mol) and compound 38 (-5.6 kcal/mol) showed good binding affinities with better docking scores among all the ligands. Amidst the produced conformations, with the amino acid residues Asn705, Gln711, Arg752, and Thr877. The binding poses of the top ligands in the active site of the human androgen receptor are depicted in figure 9. Other phytochemical compounds showed low binding affinity and the absence of hydrogen bonding. Compound 33 could be an effective anti-androgen because the hydrogen bond interacting amino acid residue (Thr877) observed in the active site of the human androgen receptor in this study was similar to the active site residues of the human androgen receptor followed on docking the piperine, which showed an antagonistic effect on dihydrotestosterone and proved to be an effective male contraceptive pill (Chinta et al., 2015). The ethanolic seed extract of bonduc was treated to male wistar rats for 60 days in dose dependent manner (200 and 400 mg/kg) to check the anti-androgenic activity and after 60 days, the sperms of rats got affected and a decrease in testosterone levels observed. There is a reduction in sperm count, motility and bulging of acrosomal membrane and detachment of sperm heads happens due to androgen deficiency. Thus, there is an action to reduce the hyperandrogenism which is a main factor for PCOS (Kandasamy and Balasundaram, 2021a).

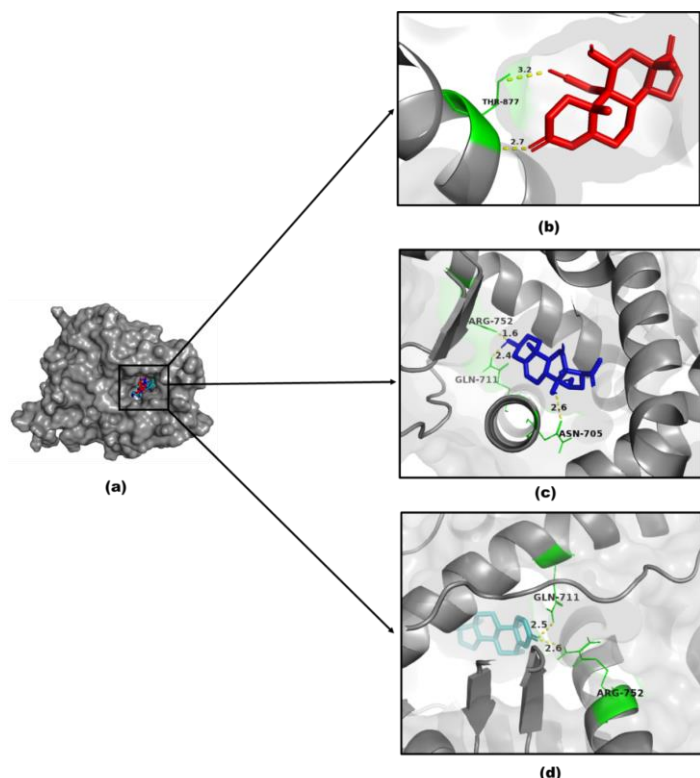


Figure 9 (a)The binding poses of compound 33 (red), compound 35 (blue) and Compound 38 (teal) to human androgen receptor (b) compound 33 interacting with the residues, Thr877 (green) forming hydrogen bonds (yellow) of length 2.7 Å and 3.2 Å, respectively (c) compound 35 interacting with the residues, Asn705, Gln711, Arg752 (green) forming hydrogen bonds (yellow) of length 2.6 Å, 2.4 Å and 1.6 Å respectively (d) Compound 38 interacting with the residues, Gln711 and Arg752 (green) forming hydrogen bonds (yellow) of length 2.5 Å and 2.6 Å.

On docking the ligands to the target estrogen receptor α , compound 33 (-8.6 kcal/mol), compound 35 (-8.0 kcal/mol), and compound 38 (-8.8 kcal/mol) represented good binding affinity with better docking score among the eight compounds. Arg394, His524 and Glu353 demonstrated hydrogen bonding. The binding poses of the top ligands in the active site of estrogen receptor α are depicted in figure 10. Compound 35 could be a better anti-estrogenic compound because the amino acid residues through which this compound interacts with the target estrogen receptor α is similar to the residues found in the active site of 4-hydroxytamoxifen - ER α interaction. 4-hydroxytamoxifen drug was prescribed for ER-positive breast cancer patients that showed an effective binding score to estrogen receptor alpha (Acharya et al., 2019). For checking the anti-estrogenic activity, the female albino rats were used and they were treated with bonduc seeds for 10 days. The results showed that there is a significant effect on follicles, reduction of weight of ovary

and uterus and endometrial degeneration occurs. These results showed that there is an anti-estrogenic activity in the bonduc seeds (Kandasamy and Balasundaram, 2021b).

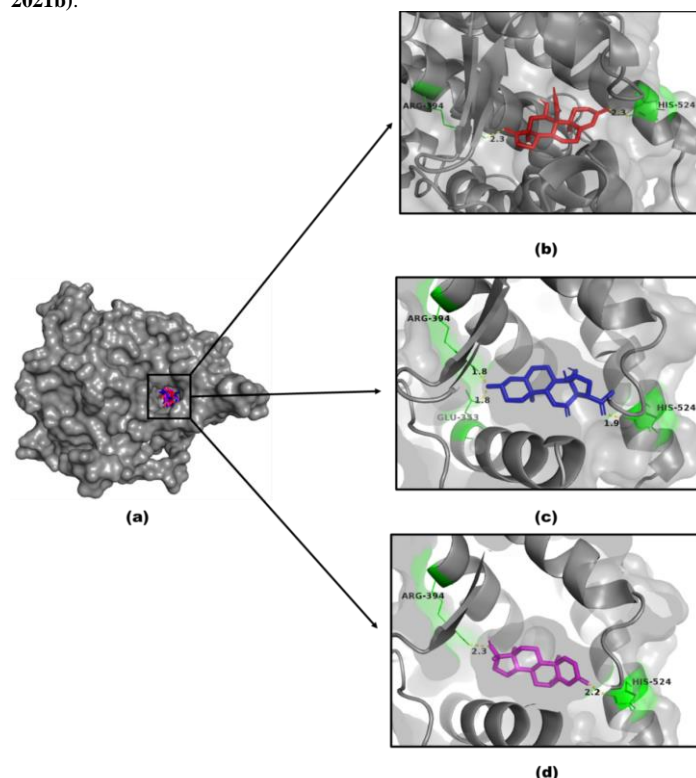


Figure 10 (a)The binding poses of compound 33 (red), compound 35 (blue) and Compound 38 (magenta) to estrogen receptor α (b) compound 33 interacting with the residues, Arg394, His524 (green) forming hydrogen bonds (yellow) of length 2.3 Å and 2.3 Å, respectively (c) compound 35 interacting with the residues, Glu353, Arg394 and His524 (green) forming hydrogen bonds (yellow) of length 1.8 Å, 1.8 Å and 1.9 Å respectively (d) Compound 38 interacting with the residues, Arg394 and His524 (green) forming hydrogen bonds (yellow) of length 2.3 Å and 2.2 Å.

Conceptual DFT

Table 4 shows the statistics of DFT-based molecular descriptors of chosen phytochemical components. Following the optimization of the eight compounds with the B3LYP method and based on molecular orbital theory, ten different descriptors were generated (Nagarajan et al., 2020a). The energies of the LUMO (ELUMO) and HOMO (EHOMO) molecular orbitals were estimated using Fukui's theory.

Table 4 DFT descriptors of the selected eight phytochemical compounds from *C. bonducella* methanol seed kernel extract

Compound number	E_T (eV)	Dipole moment (Debye)	E_H (eV)	E_L (eV)	ΔE	η	σ	χ	μ	ω
Compound 33	-39611.0893	6.8689	-6.09	-1.39	4.7	2.35	0.21	-3.74	3.74	2.97
Compound 35	-32018.5647	8.6926	-6.61	-4.7	1.91	0.95	0.52	-5.65	5.65	16.74
Compound 38	-27336.8435	2.6607	-6.29	-1.7	4.59	2.29	0.21	-3.99	3.99	3.47
Compound 39	-33570.1587	4.1165	-6.07	-1.07	5	2.5	0.2	-3.57	3.57	2.54
Compound 40	-28933.3363	12.2081	-6.32	-5.7	0.62	0.31	1.61	-6.01	6.01	58.25
Compound 41	-43303.9483	5.3895	-5.7	-5.3	0.4	0.2	2.5	-5.5	5.5	75.62
Compound 42	-23042.885	3.2057	-5.76	-0.27	5.49	2.74	0.18	-3.015	3.015	1.65
Compound 43	-36714.1638	6.4642	-6.12	-1.86	4.26	2.13	0.23	-3.99	3.99	3.73

E_T – Total Energy; E_H – HOMO; E_L – LUMO; ΔE – HOMO/LUMO Energy Gap; η – Absolute Hardness; σ – Global softness; χ – Electronegativity; μ – Chemical potential; ω – Electrophilicity.

ΔE is directly related to molecular reactivity since it represents the energy required to transfer molecules from the HOMO to the LUMO state (Yadalam et al., 2021a). Compound 41 had the lowest ΔE , while compound 42 had the highest ΔE . The narrower the energy gap, the greater the molecule's activity, which is linked to the transition of molecules from the HOMO to the LUMO state (Yadalam et al.,

2021b). Low ΔE values were also found in compounds 40 and 35. The energy gaps (E) between the HOMO and LUMO of the molecules were calculated using the difference in energies between the two orbitals: $\Delta E = ELUMO - EHOMO$ (Nagarajan et al., 2020b). Figure 11 shows electron density maps that show the density of electrons in various locations of the molecules. A molecule's chemical

reactivity is proportional to its molecular dipole moment (Yadalam et al., 2021c; Mert et al., 2011). Compound 40 has the maximum dipole moment (12.2081debye), followed by compound 35 (8.6926 debye) and compound 33 (6.8689debye). The ability of a molecule to take electrons is measured by its electronegativity. It is a crucial criterion for evaluating how effective the

molecule's inhibition is. If a molecule's electronegativity is lower, it will have a greater effect on inhibiting other molecules (Yadalam et al., 2021d). The electronegativity index of Compound 40 (-6.01) is the lowest, followed by compound 35 (-5.655) and compound 41 (-5.5). The results of conceptual DFT are compatible with the docking results of the selected compounds.

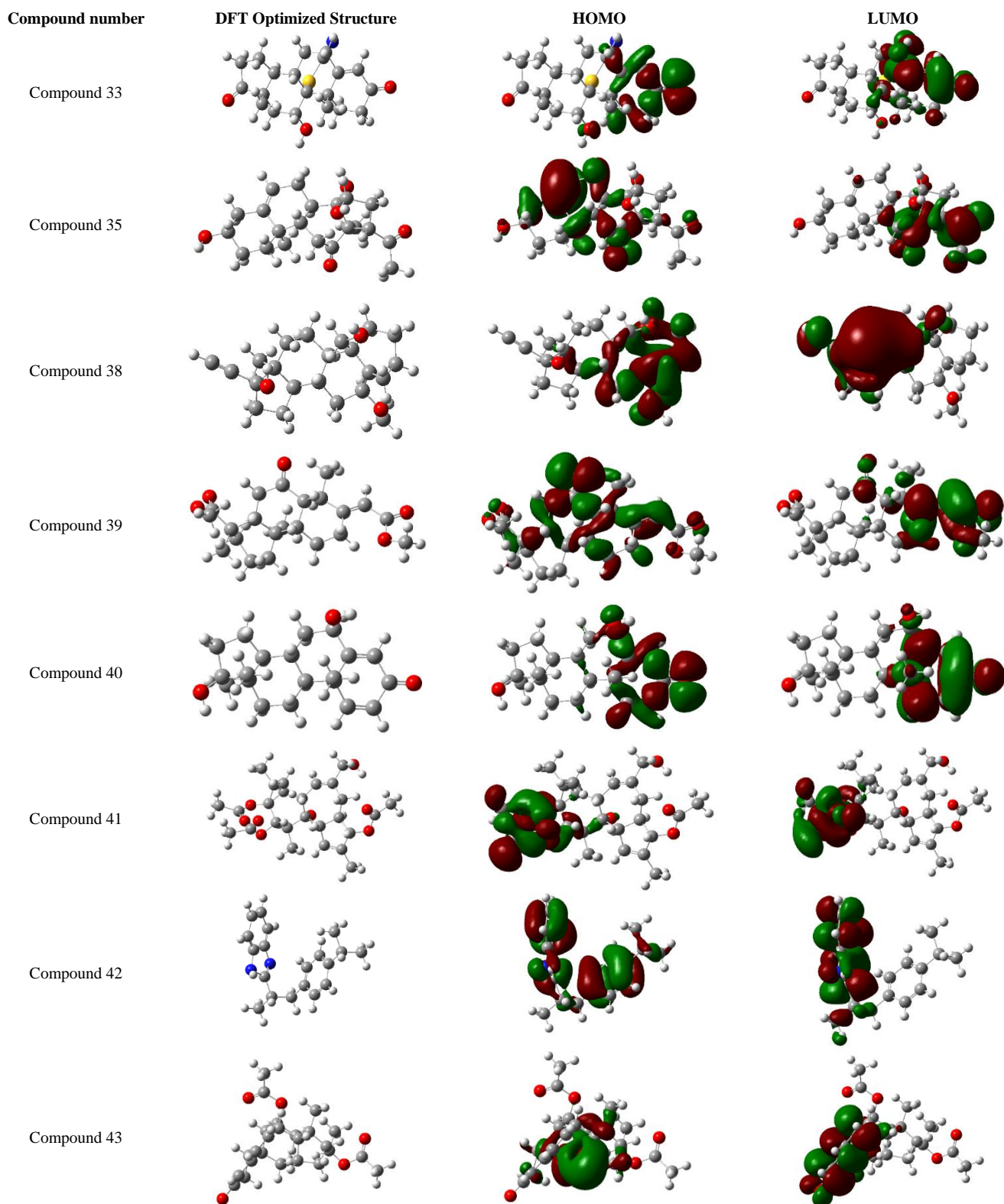


Figure 11 DFT – Electron density maps of the selected eight phytochemical compounds from methanol seed kernel extract of *C. bonducella*

ADME/T analysis

Chemical absorption, distribution, metabolism, excretion, and toxicity (ADMET) are important factors in drug discovery and development. A high-quality drug candidate should not only be effective against the therapeutic target, but it should also exhibit appropriate ADMET properties at a therapeutic dose (Guan et al., 2018). ADME/T (absorption, distribution, metabolism, excretion, and toxicity) and

physicochemical properties of the selected eight phytochemical compounds are represented in Table 5.

Table 5 ADME/T properties of the selected eight phytochemical compounds from *C. bonducella* methanol seed kernel extract

Properties	Compound 33	Compound 35	Compound 38	Compound 39	Compound 40	Compound 41	Compound 42	Compound 43
Absorption Properties								
Caco-2 Permeability (Optimal: higher than -5.15 Log unit or -4.70 or -4.80)	-4.553 cm/s	-4.944 cm/s	-4.604 cm/s	-4.531 cm/s	-4.774 cm/s	-5.131 cm/s	-4.503 cm/s	-4.606 cm/s
Human Intestinal Absorption (HIA) ≥30%: HIA+; <30%: HIA-	++ 0.753	++ 0.702	++ (0.864)	++ (0.764)	++ (0.786)	+ (0.573)	++ (0.887)	++ (0.809)
P-glycoprotein Substrate	--- 0.019	--- 0.031	--- (0.095)	--- (0.015)	--- (0.047)	- (0.304)	--- (0.07)	--- (0.031)
P-glycoprotein Inhibitor	++ 0.744	+ 0.557	--- (0.258)	++ (0.748)	- (0.363)	+ (0.536)	+ (0.5)	+++ (0.968)
Distribution Properties								
PPB (Plasma Protein Binding): 90%	88.995 %	81.22 %	80.648 %	89.608 %	70.029 %	71.754 %	92.294 %	91.436 %
Blood-Brain Barrier (BBB) BB ratio ≥0.1: BBB+; BB ratio <0.1: BBB-	++	+++	+++	+++	++	+	+++	++
VD (Volume Distribution) 0.04–20 L/kg	-0.165 L/kg	-0.311 L/kg	-0.02 L/kg	-0.157 L/kg	0.289 L/kg	0.071 L/kg	1.155 L/kg	-0.287 L/kg
Metabolism Properties								
P450 CYP1A2 inhibitor	-- (0.115)	--- (0.035)	--- (0.041)	--- (0.07)	--- (0.095)	--- (0.056)	+ (0.674)	--- (0.036)
P450 CYP1A2 Substrate	- (0.33)	- (0.33)	- (0.36)	- (0.459)	--- (0.266)	+ (0.516)	+ (0.586)	- (0.477)
P450 CYP3A4 inhibitor	--- (0.142)	--- (0.063)	--- (0.079)	--- (0.245)	- (0.448)	--- (0.22)	++ (0.749)	--- (0.19)
P450 CYP3A4 substrate	+ (0.63)	+ (0.653)	++ (0.765)	+ (0.663)	+ (0.634)	+ (0.69)	+ (0.522)	+ (0.562)
P450 CYP2C9 inhibitor	--- (0.135)	--- (0.061)	--- (0.048)	--- (0.096)	--- (0.271)	--- (0.176)	++ (0.718)	--- (0.137)
P450 CYP2C9 substrate	--- (0.243)	--- (0.267)	--- (0.118)	- (0.323)	--- (0.22)	--- (0.291)	+ (0.552)	- (0.316)
P450 CYP2C19 inhibitor	--- (0.228)	--- (0.116)	--- (0.17)	- (0.314)	- (0.318)	--- (0.098)	+ (0.687)	--- (0.179)
P450 CYP2C19 substrate	+ (0.51)	- (0.484)	+ (0.569)	+ (0.51)	- (0.485)	- (0.482)	+ (0.686)	+ (0.594)
P450 CYP2D6 inhibitor	--- (0.176)	--- (0.168)	--- (0.147)	- (0.313)	- (0.341)	- (0.352)	++ (0.777)	--- (0.267)
P450 CYP2D6 substrate	--- (0.195)	- (0.326)	--- (0.078)	--- (0.253)	--- (0.232)	--- (0.247)	- (0.451)	--- (0.267)
Excretion Properties								
T 1/2 (Half Life Time) (>8 h: high; 3 h < CI < 8 h: moderate; <3 h: low)	1.502 h	1.268 h	1.645 h	1.55 h	1.75 h	1.587 h	2.357 h	1.61 h
Toxicity Properties								
hERG (hERG Blockers)	- (0.321)	--- (0.276)	- (0.309)	- (0.447)	- (0.436)	- (0.351)	++ (0.82)	- (0.478)
AMES (Ames Mutagenicity)	--- (0.058)	--- (0.112)	--- (0.086)	--- (0.038)	--- (0.134)	+ (0.504)	+ (0.558)	--- (0.002)
DILI (Drug Induced Liver Injury)	+ (0.548)	--- (0.26)	+ (0.578)	- (0.43)	--- (0.116)	--- (0.22)	+ (0.616)	- (0.436)
Physicochemical Property								
LogS (Solubility)	11.849	200.571	26.81	6.978	31.563	31.924	1.027	2.881
	µg/mL	µg/mL	µg/mL	µg/mL	µg/mL	µg/mL	µg/mL	µg/mL
LogD7.4 (Distribution Coefficient D)	2.995	1.837	2.802	2.147	2.884	2.381	3.359	3.565
LogP (Distribution Coefficient P)	3.395	1.78	3.016	3.707	2.991	2.319	4.551	4.404

Here, selected eight phytocompounds have shown good human intestinal absorption (HIA) and Caco-2 permeability values. ADME/T is a critical parameter for determining a compound's fate when taken orally. *In vitro* permeability studies are commonly done in the Caco-2 cell line, which resonates the compound's intestinal absorption (Natesh et al., 2021). Following absorption, compounds travel via the bloodstream to different regions of the body before being processed in the liver. Cytochrome P450 family containing a set of enzymes can break down ingested drug molecules in the liver and remove them through bile and urine (Glue and Clement, 1999).

Here, we found that compounds (33, 35, 38, 39, 40, 41 and 43) can easily metabolise cytochrome P450 family enzyme. Selected eight phytochemical compounds shows that less than 3 hours it denotes the lower level of half-life and these compounds easily eliminate from our body. The criteria that high biological activity through lower toxicity of compounds elementary condition for drug discovery process. The phytochemical compounds contain a high level of oral acute toxicity and carcinogenicity to eliminate for future study (Rahman et al., 2021). Toxicity evaluation of selected phytochemical compounds prediction represents that except compound 42, all the other compounds (33, 35, 38, 39, 40, 41 and 43) are non-blockers of hERG and there is no cardiac side effect in humans. AMES (Ames Mutagenicity) shows that six compounds (33, 35, 38, 39, 40 and 43) respond to non-mutagenicity and did not cause any genetic damage.

CONCLUSION

PCOS is a heterogeneous disorder with life-threatening long-term complications. Therefore, this health issue should be addressed immediately using alternate therapies in this study, seed kernels of *C. bonducella* was screened for potential

anti-estrogenic and anti-androgenic phytochemical compounds by computational analysis. The results of this study suggest that the phytochemical compounds (33, 35, 38, 40 and 43) showed good binding affinities to the targets human aromatase (*CYP19A1*), human 17β-hydroxysteroid dehydrogenase type 1 (*HSD17b1*), human androgen and estrogen receptor α) of ovarian steroidogenesis pathway. Hence, these compounds could be recommended as anti-estrogenic and anti-androgenic drugs in the management of PCOS. On the whole, the current study provides valuable insights and opens the door to new research opportunities for the exploration of the phytochemical compounds in *in vitro* and *in vivo* PCOS models.

Conflict of interest The authors declare that they have no conflict of interest.

Acknowledgement Authors thank High-Performance Computing Center, SRM Institute of Science and Technology for providing the computational facility.

REFERENCE

Acharya, R., Chacko, S., Bose, P., Lapenna, A., & Pattanayak, S. P. (2019). Structure based multitargeted molecular docking analysis of selected furanocoumarins against breast cancer. Scientific reports, 9(1), 1-13. <https://doi.org/10.1038/s41598-019-52162-0>
 Ashraf, Z., Saeed, A., & Nadeem, H. (2014). Design, synthesis and docking studies of some novel isocoumarin analogues as antimicrobial agents. RSC Advances, 4(96), 53842-53853. <https://doi.org/10.1039/c4ra07223e>
 Bouzekri, O., Elgamouz, S., Ghaleb, A., Amechrouq, A., El Drissi, M., & Choukrad, M. (2022). Valorization of perillaldehyde molecule contained in the essential oil of *Anmodaucus Leucotrichus* Coss. from the saharan zones of

- morocco. Journal of Microbiology, Biotechnology and Food Sciences, 11(4), e4324. <https://doi.org/10.55251/jmbfs.4324>
- Boyle, J. A., & Teede, H. J. (2016). Refining diagnostic features in PCOS to optimize health outcomes. Nature Reviews Endocrinology, 12(11), 630-631. <https://doi.org/10.1038/nrendo.2016.157>
- Chinta, G., Charles, M. R. C., Klopčič, I., Dolenc, M. S., Periyasamy, L., & Coumar, M. S. (2015). In silico and in vitro investigation of the piperine's male contraceptive effect: docking and molecular dynamics simulation studies in androgen-binding protein and androgen receptor. Planta Medica, 81(10), 804-812. <https://doi.org/10.1055/s-0035-1546082>
- Conway, G., Dewailly, D., Diamanti-Kandaraki, E., Escobar-Morreale, H. F., Franks, S., Gambineri, A., & Yildiz, B. O. (2014). The polycystic ovary syndrome: a position statement from the European Society of Endocrinology. European journal of endocrinology, 171(4), P1-P29. <https://doi.org/10.1530/EJE-14-0253>
- CYP19A1 cytochrome P450 family 19 subfamilies A member 1 [Homo sapiens (human)] [database on the Internet]. 2018. Available from <https://www.ncbi.nlm.nih.gov/gene/1588> (Accessed May 2021)
- Dallakyan, S., & Olson, A. J. (2015). Small-molecule library screening by docking with PyRx. In Chemical biology (pp. 243-250). Humana Press, New York, NY. https://doi.org/10.1007/978-1-4939-2269-7_19
- Dokras, A., Saini, S., Gibson-Helm, M., Schulkin, J., Cooney, L., & Teede, H. (2017). Gaps in knowledge among physicians regarding diagnostic criteria and management of polycystic ovary syndrome. Fertility and sterility, 107(6), 1380-1386. <https://doi.org/10.1016/j.fertnstert.2017.04.011>
- Glue, P., & Clement, R. P. (1999). Cytochrome P450 enzymes and drug metabolism—basic concepts and methods of assessment. Cellular and molecular neurobiology, 19(3), 309-323. <https://doi.org/10.1023/A:1006993631057>
- Guan, L., Yang, H., Cai, Y., Sun, L., Di, P., Li, W., Liu, G., & Tang, Y. (2018). ADMET-score - a comprehensive scoring function for evaluation of chemical drug-likeness. MedChemComm, 10(1), 148-157. <https://doi.org/10.1039/c8md00472b>
- Holzer, H., Casper, R., & Tulandi, T. (2006). A new era in ovulation induction. Fertility and sterility, 85(2), 277-284. <https://doi.org/10.1016/j.fertnstert.2005.05.078>
- Homburg, R. (2005). Clomiphene citrate—end of an era? A mini-review. Human reproduction, 20(8), 2043-2051. <https://doi.org/10.1093/humrep/dei042>
- Hooijerink, D., Schilt, R., Hoogenboom, R., & Huvencers-Oorsprong, M. (1998). Identification of metabolites of the anabolic steroid methandienone formed by bovine hepatocytes in vitro. Analyst, 123(12), 2637-2641. <https://doi.org/10.1039/a805132a>
- HSD17B1 hydroxysteroid 17-beta dehydrogenase 1 [Homo sapiens (human)] [database on the Internet]. 2016. Available from <https://www.ncbi.nlm.nih.gov/gene/3292> (Accessed May 2021)
- Hu, Z., Chen, J. T., Jiang, S. C., Liu, Z., Ge, S. B., & Zhang, Z. (2020). Chemical components and functions of Taxus chinensis extract. Journal of King Saud University-Science, 32(2), 1562-1568. <https://doi.org/10.1016/j.jksus.2019.12.012>
- Iftikhar, H., Ahmed, D., & Qamar, M. T. (2019). Study of phytochemicals of *Melilotus indicus* and alpha-amylase and lipase inhibitory activities of its methanolic extract and fractions in different solvents. ChemistrySelect, 4(26), 7679-7685. <https://doi.org/10.1002/slct.201901120>
- Iheagwam, F. N., Ogunlana, O. O., Ogunlana, O. E., Isewon, I., & Oyelade, J. (2019). Potential anti-cancer flavonoids isolated from *Caesalpinia bonduc* young twigs and leaves: molecular docking and in silico studies. Bioinformatics and Biology Insights, 13, 1177932218821371. <https://doi.org/10.1177/1177932218821371>
- Janani, D. M., & Usha, B. (2020). In silico analysis of functional non-synonymous and intronic variants found in a polycystic ovarian syndrome (PCOS) candidate gene: *DENNDIA*. Indian J. Biochem. Biophys. 57, 584-593.
- Kandasamy, V., & Balasundaram, U. (2021). *Caesalpinia bonduc* (L.) Roxb. As a promising source of pharmacological compounds to treat Poly Cystic Ovary Syndrome (PCOS): A review. Journal of Ethnopharmacology, 279, 114375. <https://doi.org/10.1016/j.jep.2021.114375>
- Khare, C.P., 2007. *Launaea pinnatifida* Cass. Indian Med. Plants 1-1. https://doi.org/10.1007/978-0-387-70638-2_887
- Kitchen, D. B., Decornez, H., Furr, J. R., & Bajorath, J. (2004). Docking and scoring in virtual screening for drug discovery: methods and applications. Nature reviews Drug discovery, 3(11), 935-949. <https://doi.org/10.1038/nrd1549>
- Kulkarni, S. A., Nagarajan, S. K., Ramesh, V., Palaniyandi, V., Selvam, S. P., & Madhavan, T. (2020). Computational evaluation of major components from plant essential oils as potent inhibitors of SARS-CoV-2 spike protein. Journal of Molecular Structure, 1221, 128823. <https://doi.org/10.1016/j.molstruc.2020.128823>
- Kumavath, R., Azad, M., Devarapalli, P., Tiwari, S., Kar, S., Barh, D., & Kumar, A. P. (2016). Novel aromatase inhibitors selection using induced fit docking and extra precision methods: Potential clinical use in ER-alpha-positive breast cancer. Bioinformation, 12(6), 324.
- Lerchbaum, E., Schwetz, V., Rabe, T., Giuliani, A., & Obermayer-Pietsch, B. (2014). Hyperandrogenemia in polycystic ovary syndrome: exploration of the role of free testosterone and androstenedione in metabolic phenotype. PLoS One, 9(10), e108263. <https://doi.org/10.1371/journal.pone.0108263>
- Jordaan, M. A., Ebenezer, O., Damoyi, N., & Shapi, M. (2020). Virtual screening, molecular docking studies and DFT calculations of FDA approved compounds similar to the non-nucleoside reverse transcriptase inhibitor (NNRTI) efavirenz. Heliyon, 6(8), e04642. <https://doi.org/10.1016/j.heliyon.2020.e04642>
- Meerwal, P., & Jain, G. C. (2016). Antifertility effect of *Caesalpinia bonducella* (L.) Fleming in male Wistar rat. International Journal of Pharmacognosy, 3(6), 265-275. [https://doi.org/10.13040/ijpsr.0975-8232.ijp.3\(6\).265-75](https://doi.org/10.13040/ijpsr.0975-8232.ijp.3(6).265-75)
- Meier, R. K. (2018). Polycystic ovary syndrome. Nursing Clinics, 53(3), 407-420. <https://doi.org/10.1016/j.cnur.2018.04.008>
- Mert, B. D., Mert, M. E., Kardaş, G., & Yazıcı, B. (2011). Experimental and theoretical investigation of 3-amino-1, 2, 4-triazole-5-thiol as a corrosion inhibitor for carbon steel in HCl medium. Corrosion science, 53(12), 4265-4272. <https://doi.org/10.1016/j.corsci.2011.08.038>
- Nagarajan, S. K., Babu, S., Sohn, H., & Madhavan, T. (2020). Molecular-level understanding of the somatostatin receptor 1 (SSTR1)-ligand binding: a structural biology study based on computational methods. ACS omega, 5(33), 21145-21161. <https://doi.org/10.1021/acscomega.0c02847>
- Natesh, J., Mondal, P., Penta, D., Salam, A. A. A., & Meeran, S. M. (2021). Culinary spice bioactives as potential therapeutics against SARS-CoV-2: Computational investigation. Computers in biology and medicine, 128, 104102. <https://doi.org/10.1016/j.combiomed.2020.104102>
- O'Boyle, N. M., Banck, M., James, C. A., Morley, C., Vandermeersch, T., & Hutchison, G. R. (2011). Open Babel: An open chemical toolbox. Journal of cheminformatics, 3(1), 1-14.
- Panwar, U., & Singh, S. K. (2021). In silico virtual screening of potent inhibitor to hamper the interaction between HIV-1 integrase and LEDGF/p75 interaction using E-pharmacophore modeling, molecular docking, and dynamics simulations. Computational Biology and Chemistry, 93, 107509. <https://doi.org/10.1016/j.compbiolchem.2021.107509>
- Rodriguez Paris, V., & Bertoldo, M. J. (2019). The mechanism of androgen actions in PCOS etiology. Medical sciences, 7(9), 89. <https://doi.org/doi:10.3390/medsci7090089>
- Rahman, M. M., Biswas, S., Islam, K. J., Paul, A. S., Mahato, S. K., Ali, M. A., & Halim, M. A. (2021). Antiviral phytochemicals as potent inhibitors against NS3 protease of dengue virus. Computers in Biology and Medicine, 134, 104492. <https://doi.org/10.1016/j.combiomed.2021.104492>
- Ridho, M. R., Setiawan, A., Sarno, S., Arwingsyah, A., Patriono, E., & Sulistiono, S. (2020). Bioactive Compounds Evaluation of the Mudskippers in the Estuarine Area of Musi River, South Sumatera, Indonesia. Journal of Ecological Engineering (JEE), 21(3), 70-80. <https://doi.org/10.12911/22998993/118296>
- Sachan, N. K., Verma, S., Sachan, A. K., & Arshad, H. (2010). An investigation to antioxidant activity of *Caesalpinia bonducella* seeds. Ann. Pharm. & Pharm. Sci; Vol, 1, 2.
- Salunke, K. R., Ahmed, R. N., & Marigoudar, S. R. (2011). Effect of graded doses of *Caesalpinia bonducella* seed extract on ovary and uterus in albino rats. <https://doi.org/10.1515/JBCPP.2011.006>
- Sarma, G., & Das, S. (2018). The hypolipidemic activity of ethanolic extract of seed kernel of *Caesalpinia bonducella* fleming on serum lipids and atherogenesis in albino rats fed with high fat diet. <https://doi.org/http://dx.doi.org/10.18203/2319-2003.ijbcp20180096>
- Satoh, D., & Morita, J. (1968). Studies on Digitalis Glycosides. The Structure of Purprogenin. Chemical and Pharmaceutical Bulletin, 16(1), 178-180.
- Shukla, S., Mehta, A., John, J., Singh, S., Mehta, P., & Vyas, S. P. (2009). Antioxidant activity and total phenolic content of ethanolic extract of *Caesalpinia bonducella* seeds. Food and chemical Toxicology, 47(8), 1848-1851. <https://doi.org/10.1016/j.fct.2009.04.040>
- Shukla, S., Mehta, A., Mehta, P., Vyas, S. P., Shukla, S., & Bajpai, V. K. (2010). Studies on anti-inflammatory, antipyretic and analgesic properties of *Caesalpinia bonducella* F. seed oil in experimental animal models. Food and Chemical Toxicology, 48(1), 61-64. <https://doi.org/10.1016/j.fct.2009.09.015>
- Sidra, S., Tariq, M. H., Farrukh, M. J., & Mohsin, M. (2019). Evaluation of clinical manifestations, health risks, and quality of life among women with polycystic ovary syndrome. PLoS One, 14(10), e0223329. <https://doi.org/10.1371/journal.pone.0223329>
- Singla, R., & Jaitak, V. (2015). Molecular docking simulation study of phytoestrogens from *Asparagus racemosus* in breast cancer progression. International Journal of Pharmaceutical Sciences and Research, 6(1), 172. [https://doi.org/10.13040/IJPSR.0975-8232.6\(1\).172-82](https://doi.org/10.13040/IJPSR.0975-8232.6(1).172-82)
- Stouten, P.F.W., Kroemer, R.T., (2006). Docking and scoring. Compr. Med. Chem. II 4, 255-279. <https://doi.org/10.1016/b0-08-045044-x/00253-4>
- Trott, O., & Olson, A. J. (2010). AutoDock Vina: improving the speed and accuracy of docking with a new scoring function, efficient optimization, and multithreading. Journal of computational chemistry, 31(2), 455-461. <https://doi.org/10.1002/jcc.21334>
- Veira, T. F., & Sousa, S. F. (2019). Comparing AutoDock and Vina in ligand/decoy discrimination for virtual screening. Applied Sciences, 9(21), 4538. <https://doi.org/10.3390/app9214538>
- Xu, X. L., Deng, S. L., Lian, Z. X., & Yu, K. (2021). Estrogen receptors in polycystic ovary syndrome. Cells, 10(2), 459. <https://doi.org/10.3390/cells10020459>

Yadalam, P. K., Varatharajan, K., Rajapandian, K., Chopra, P., Arumuganainar, D., Nagarathnam, T.,... & Madhavan, T. (2021). Antiviral essential oil components against SARS-CoV-2 in pre-procedural mouth rinses for dental settings during COVID-19: A computational study. *Frontiers in Chemistry*, 9, 86. <https://doi.org/10.3389/fchem.2021.642026>